

# Double-Machine-Learning-Based Resource Scheduling Method for Offloading Transfers

Xiao Lin\*, Songlei Lin\*, Yaping Li\*, Junyi Shao<sup>†</sup>, Keqin Shi<sup>†</sup>, Yajie Li<sup>‡</sup>

\*College of Physics and Information Engineering,

Fuzhou University, Fuzhou, China, {linxiaocer,211120098,201120072}@fzu.edu.cn

<sup>†</sup>State Key Laboratory of Advanced Optical Communication Systems and Networks, Shanghai Jiao Tong University, Shanghai, China, {shaojunyi,keqinshi}@sjtu.edu.cn

<sup>‡</sup>State Key Laboratory of Information Photonics and Optical Communications, Beijing University of Posts and Telecommunications, Beijing, China, yajieli@bupt.edu.cn

**Abstract**—Dynamically scheduling the bandwidth based on the traffic variation is important for a task offloading system. However, it faces two challenges. On one hand, the time-varying nature of the offloading traffic makes it difficult to be predicted accurately. On the other hand, differentiated mechanisms are applied to different offloading task types, which greatly complicates the behavior of the task offloading system. It is hence difficult to estimate the performance metrics accurately, especially when the metric values are extremely small. To tackle this, we present a double-machine-learning-based resource scheduling (DML-RS) method for task offloading traffic in this paper. The features of DML-RS are as follows: i) the wavelet transform and the sliding time window are incorporated with the LSTM traffic prediction model, which can capture the periodic and volatile natures of the offloading traffic and hence improve the prediction accuracy; ii) the logarithmic converting is applied to the ANN estimation models, which can improve the sensitivity of the ANN models to the small values and hence provides higher estimation accuracy. As a result, DML-RS can predict the traffic demand of the next network reconfiguration time point and optimize the resource allocation based on the performance estimations in advance. Results show that DML-RS offers near-optimal results compared with the existing method.

**Index Terms**—Optical networks, traffic prediction, performance estimation, network optimization, artificial neural network, multi-access edge computing.

## I. INTRODUCTION

Over the last few years, Multi-Access Edge Computing (MEC) has empowered the network edge. MEC servers are deployed in close proximity to user equipment (UE) in order to improve the quality of service (QoS) and enhance the quality of experience (QoE) [1]. However, MEC servers often face overload issues, since they are constrained in computing power and storage capacity [2]. As a result, task offloading between geo-distributed MEC servers is necessary, which has created the need for data transfers from one MEC server to another. However, the explosive growth of offloading traffic, fueled by emerging MEC applications like Tactile Internet, smart cities and hologram, imposes a great challenge on the network infrastructure of the task offloading system [3].

As an emerging optical transmission technology, elastic optical network (EON) is advantageous for the low-latency,

small-overhead and high-bandwidth features of optical connections. The modulation format and data rate of an EON connection can be adapted according to the heterogeneous requirements of offloading transfers. It is hence desirable to carry the offloading traffic. However, EON needs to establish an end-to-end lightpath before sending the data, which may take hundreds of milliseconds [4]. To minimize such establishment overhead, a portion of the link capacity has to be pre-reserved for offloading traffic. This may lead to the bandwidth contention between the offloading traffic and background traffic, especially at peak hours. On the other hand, MEC operators often purchase link bandwidth from ISP providers based on peak demand. To accommodate the growing peak demand, MEC operators have to constantly purchase link bandwidth even if the average utilization is low [5]. The increasing offloading transfers not only provoke the bandwidth contention, but also incur expensive transfer cost. Consequently, the efficient use of the bandwidth resources is technically and economically important for MEC operators.

Prior studies proposed novel allocation schemes, flexible scheduling methods and efficient provisioning policies to maximize the utilization, minimize the cost and guarantee the delay constraint [1]–[6]. In essence, the prior studies focused on a certain type of fixed load or a set of given transfer requests and formulated their resource allocation problems as static optimization problems. In practice, the offloading traffic varies dynamically throughout the day [7]. For example, the traffic in an enterprise network often peaks at the work-hours, but falls quickly in the evening. While the prior studies have been proven to be effective for the static traffic, they find it difficult to handle the dynamic traffic. A static allocation scheme may either waste a large amount of bandwidth resources when the traffic is low, or be vulnerable to degraded QoS when the traffic is high. Thus, it is necessary to dynamically schedule the resources with the traffic variation.

Intuitively, the efficiency of dynamic resource scheduling depends on two key factors: (a) how to predict the traffic variation accurately; (b) how to estimate the network performance based on the traffic and resource allocation accurately. Our observations on the key factors are threefold as follows.

First, as previously mentioned, the traffic is periodic at the

This work was supported by the National Natural Science Foundation of China (61901118 and 61901053).

day granularity. However, at a finer time granularity, the traffic is highly volatile due to the stochastic behavior of the end users. The existing methods are capable of providing traffic prediction information at a relatively coarse level. While the coarse-grained prediction is sufficient enough for a long-term network planning, most methods find it difficult to provide highly accurate predictions for dynamic scheduling at a finer time granularity [8]. The periodic and volatile natures of the offloading traffic impose a challenge on the existing traffic prediction methods.

Second, the offloading traffic is often a mix of multiple types with different characteristics and requirements. Differentiated mechanisms hence are applied to different traffic types. For instance, preemption and resource partitioning mechanisms were used to handle a mix of elephant and mice traffic [6]. In [7], preemption, resource partitioning and temporary storage mechanisms were used to handle a mix of delay-tolerant (DT) and delay-sensitive (DS) traffic. Unfortunately, the co-existence of multiple mechanisms complicates the behavior of the task offloading system. It is challenging to estimate how the performance metrics change with the traffic and resource allocation efficiently. In other words, the conventional estimation methods may be either time-consuming (like the discrete event simulation) or not accurate enough (like the Erlang fixed point approximation).

Third, MEC applications often have the stringent performance requirements, which suggests the value of the network performance metric could be extremely small in certain cases, such as  $10^{-5}$  blocking probability in [9]. Such small values can lead to a vanishing gradient issue as well as unacceptable estimation error when using the conventional estimation methods. As a result, the conventional estimation methods have difficulty in achieving high accuracy.

In this work, we consider the task offloading system interconnected by the EON link [7], and explore how to dynamically schedule the resources in advance based on the traffic prediction. Our contributions are summarized as follows:

- 1) We present a long short-term memory (LSTM) model, which is enhanced by the sliding time window and the wavelet analysis to learn the fluctuation, periodic and volatile characteristics from the historical traffic data. Experiments show that the LSTM model is more accurate than the conventional prediction model.
- 2) We present artificial neural network (ANN) models to learn the impacts of the traffic and resource allocation on the network performance metrics. To overcome the vanishing gradient issue, the logarithmic functions are used to convert the values of the metrics into the logarithmic forms. The ANN models hence are more sensitive to the extremely small values than the conventional models learning from the original values. Experiments show that the ANN models have higher estimation accuracy and shorter training time than the conventional models especially when the metrics vary from  $10^{-10}$  to  $10^{-5}$ .
- 3) We present a double-machine-learning-based resource scheduling method (DML-RS), whose main ideas are

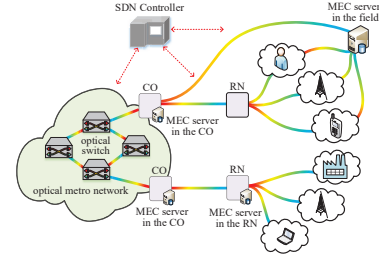


Fig. 1: The illustration of the network infrastructure.

threefold as follows. i) DML-RS uses the LSTM model to predict the traffic demand at the next network re-configuration time. ii) DML-RS formulates the resource scheduling problem for the next reconfiguration time as an optimization model, which aims to minimize the performance metrics while improving the bandwidth utilization. iii) To find the optimal result, DML-RS searches feasible resource allocations and estimates their corresponding performance using the ANN models. Simulations show that DML-RS can meet the constraints while improving the utilization efficiently, compared with the existing methods.

The rest of this paper is organized as follows: Sect. II describes the system model. Sect. III and Sect. IV illustrate the LSTM model and the ANN models, respectively. Sect. V presents DML-RS, which is followed by the evaluation in Sect. VI. Finally, Sect. VII concludes this paper.

## II. SYSTEM MODEL

### A. Network Architecture

The task offloading system over the point-to-point (P2P) EON link [7] is considered. The network infrastructure is depicted in Fig. 1. The SDN controller centrally schedules and orchestrates the bandwidth resources in the EON and the storage resources in MEC servers. MEC servers can be deployed in the field, remote node (RN) and central office (CO) [10]. Our work can be applied to two P2P offloading scenarios. In the first scenario, an MEC server in the field is connected to the client networks and an MEC server in the nearest CO via the additional installed fiber links. The field server is in close proximity to the client networks and can offload its tasks to the CO server when it is overloaded. In the second scenario, an MEC server in the RN can communicate with the client networks via the existing fiber links between the client networks and the RN. Similarly, the RN server can offload its tasks to the CO server. The former offers lower transmission latency, whereas the latter is more economical.

### B. Overview

As in [7], the offloading tasks are categorized into DS tasks (e.g., Tactile Internet) and DT tasks (e.g., edge caching). To meet the low-delay requirement, DS traffic is given preemptive priority over DT traffic. To reduce peak demand, the delay tolerance of DT traffic is exploited. The storage of MEC

server is used to temporarily store DT traffic when the link is busy. To balance the bandwidth contention between DS and DT traffic and the bandwidth utilization, the link spectrum resources are partitioned into two exclusive zones and a shared zone. The exclusive zones are dedicated for DS and DT traffic, respectively. The shared zone can be used by both traffic types. In this work, we aim to dynamically adapt the bandwidth and storage resources reserved for the offloading traffic as well as the resource partitioning between DS and DT traffic based on the predicted traffic demands and the estimated performance.

The total spectrum resources are divided into frequency slots (FSs). The capacity of each FS ( $B$ ) is 12.5 GHz. Let  $n$  denote the number of FSs assigned to each task. Let  $m$  denote the modulation level assigned to each task, where  $\{m|m \in M\}$  and  $M = \{1, 2, 3\}$ .  $M$  represents the three modulation formats: BPSK, QPSK and 8QAM, respectively. The modulation level should be selected based on the transmission distance of a lightpath. Specifically, BPSK, QPSK and 8QAM support 240 km, 120 km and 60 km, respectively. Let  $H$  denote the physical distance between the MEC servers.

Tasks randomly arrive at a field/RN server and are offloaded to the CO server with a Poisson process and  $\lambda$  tasks per unit time. Task file is exponentially distributed with a service rate  $\mu$  tasks per unit time, where  $\mu = (n \cdot B \cdot m)/F$ . Let the percentage of DS traffic on all the offloading traffic be  $\delta$ . The arrival rate for DS tasks is equal to  $\lambda \cdot \delta$ . The arrival rate for DT tasks is equal to  $\lambda \cdot (1 - \delta)$ . The amounts of spectrum resources assigned to DS and DT tasks are  $c_{ds}$  and  $c_{dt}$ , respectively. The amount of spectrum resources shared by both task types is  $c_s$ . The amount of storage assigned to DT tasks is  $s$  Gb.

Upon a DS task arrival, it will be admitted when either  $c_{ds}$  or  $c_s$  has the required resources. It will preempt an active DT task in  $c_s$  when neither  $c_{ds}$  nor  $c_s$  has the required resources. It will be blocked when the spectrum resources in  $c_{ds}$  and  $c_s$  are insufficient and all the active tasks in  $c_s$  are DS.

Upon a DT task arrival, it will be admitted when either  $c_{dt}$  or  $c_s$  has the required resources. It will be stored when neither  $c_{dt}$  nor  $c_s$  has the required resources, but  $s$  is sufficient. It will be blocked when the resources in  $c_{ds}$ ,  $c_s$  and  $s$  are insufficient.

$B_{ds}$  and  $B_{dt}$  are defined as the blocking probability of DS and DT tasks, respectively.  $P_{dt}$  is defined as the preemption probability of DT tasks.  $U$  is defined as the spectrum utilization. Thus, how to decide  $c_s$ ,  $c_{ds}$ ,  $c_{dt}$  and  $s$  (i.e., the resource scheduling problem) is critical for the performance of the offloading system.

### III. LSTM-BASED TRAFFIC PREDICTION

As the EON network will be reconfigured periodically, we present an LSTM model to predict the task arrival rate at each reconfiguration time point. To enhance the LSTM model, our main ideas are twofold: i) the sliding time window (Win) is used to capture the fluctuation characteristic from the historical traffic data; ii) the wavelet analysis (Wavelet) is used to extract the periodic and volatile characteristics from the traffic data.

We first illustrate how to generate the training samples. The Internet traffic dataset collected in [11] is used to emulate

TABLE I: Traffic Prediction Performance

	MAE	MAPE (%)	MSE
ARIMA	$7.2 \cdot 10^{-2}$	2.8	$1.1 \cdot 10^{-2}$
LSTM (only Win)	$6.9 \cdot 10^{-2}$	2.7	$9.1 \cdot 10^{-3}$
LSTM (only Wavelet)	$5.8 \cdot 10^{-2}$	2.2	$6.5 \cdot 10^{-3}$
LSTM (Wavelet+Win)	$3.2 \cdot 10^{-2}$	1.2	$2.0 \cdot 10^{-3}$

the fluctuation of  $\lambda$  over time. We use consecutive traffic data points to form a Win. Besides, we use the wavelet transform to decompose each data point into an approximation component that captures the periodic characteristic and the detail components that capture the volatile characteristics. Let  $\lambda_t$  denote the task arrival rate at the reconfiguration time point  $t$ . Consider  $\lambda_t$  as the output label of a training sample. Let  $\lambda_{t-5}, \dots, \lambda_{t-1}$  form a five-entry Win. We use Symlets wavelet function and Mallat algorithm to perform a three-level decomposition on  $\lambda_{t-1}$ , which returns the approximation component  $c_{t-1}^3$  and the three detail components  $d_{t-1}^1, d_{t-1}^2, d_{t-1}^3$ . Finally, the Win from  $t-5$  to  $t-1$ , the one approximation and three detail components of  $\lambda_{t-1}$  form the nine-entry input vector of the training sample.

Our LSTM model consists of a nine-neuron input layer, a hidden layer with sixty-four neurons, and a one-neuron output layer. The MSE function is used as the loss function. The activation functions for the hidden layer are the sigmoid and tanh functions by default. The linear activation function is used for the output layer. Besides, Adam optimizer with default parameters is used in training. 80% of the dataset is used as the training set and the remaining 20% is used as the test set. During the training process, 15% of the training samples are used as the validation set to avoid over-fitting. An early stopping criterion is used to achieve faster convergence and termination. The training will be stopped when the validation loss cannot keep decreasing over 100 epochs.

To test the prediction performance, the mean absolute error

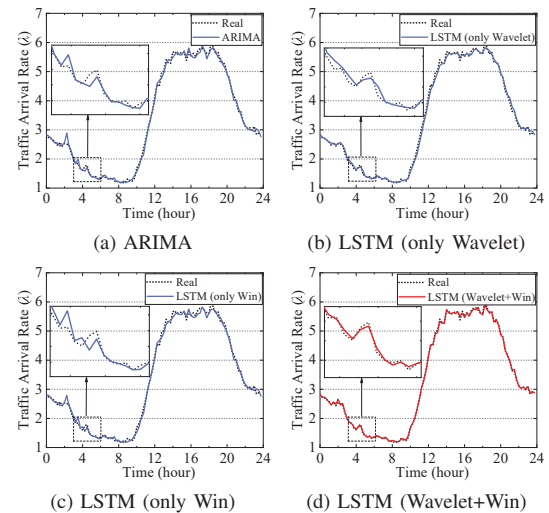


Fig. 2: The traffic predictions using different models.



(MAE), the mean absolute percentage error (MAPE) and the MSE functions are used. The autoregressive integrated moving average (ARIMA) model, the LSTM model using only the wavelet analysis and the LSTM model using only the Win are compared with our LSTM model. In Table I, our LSTM model obtains better performance than the three models in terms of the MAE, MAPE and MSE. Fig. 2 compares the predictions to the real traffic. The prediction results using the other three models may lag behind the real traffic when the real traffic is bursty. On the contrary, our LSTM model is more accurate than the others, especially when the real traffic is bursty.

#### IV. ANN-BASED PERFORMANCE ESTIMATION

As mentioned in Sect. II-B, the four metrics, i.e.,  $B_{ds}$ ,  $B_{dt}$ ,  $P_{dt}$  and  $U$ , can be used to evaluate the performance of the offloading system. Due to the complicated nature of the system behavior, we use the ANN models to estimate the metrics instead of deriving close-form approximations.

Since the values of the metrics are in the range of 0 to 1, the ANN models with the sigmoid activation functions are sufficient enough to estimate the metrics. However, the stringent performance requirements imposed by MEC applications result in the extremely small values of the performance metrics. In this case, the conventional ANN models may face the vanishing gradient issue and suffer from significant estimation error. To tackle this issue, our idea is to convert the original values of the metrics into their logarithmic forms before the training. As a result, the ANN models can be more sensitive to such extremely small values.

To generate the training samples, we run extensive simulations to collect the corresponding performance metrics under certain traffic and resource allocation conditions. Specifically,  $\lambda$ ,  $\delta$ ,  $\mu$ ,  $c_s$ ,  $c_{ds}$ ,  $c_{dt}$  and  $s$  form the seven-entry input vector of a training sample. Besides,  $\lg(B_{ds})$ ,  $\lg(B_{dt})$ ,  $\lg(P_{dt})$  and  $U$  are the output labels of the training sample. Note that  $B_{ds}$ ,  $B_{dt}$  and  $P_{dt}$  will be converted into the logarithmic forms (the base 10 logarithm function, i.e.,  $\lg(\cdot)$ ) before the training, while  $U$  remains its original form in training. This is because the values of  $U$  are larger than  $10^{-1}$  in typical network scenarios. In this case, the conventional ANN model can estimate  $U$  accurately.

Three ANN models are used to estimate  $\lg(B_{ds})$ ,  $\lg(B_{dt})$  and  $\lg(P_{dt})$ , respectively. Each model consists of a seven-neuron input layer, one hidden layer with 1500 neurons, and

TABLE II: Comparisons of Estimation Performance

		MAE	MAPE (%)	MSE	$t_{train}$ (s)
Orig-ANN	$B_{ds}$	$1.5 \cdot 10^{-3}$	$2.2 \cdot 10^3$	$1.6 \cdot 10^{-5}$	3430
	$B_{dt}$	$3.0 \cdot 10^{-3}$	$5.6 \cdot 10^3$	$3.7 \cdot 10^{-5}$	5801
	$P_{dt}$	$8.0 \cdot 10^{-4}$	$3.4 \cdot 10^3$	$2.8 \cdot 10^{-6}$	5627
	$U$	$1.6 \cdot 10^{-3}$	0.6	$5.6 \cdot 10^{-6}$	2647
Log-ANN	$B_{ds}$	$1.9 \cdot 10^{-3}$	4.7	$3.0 \cdot 10^{-4}$	1797
	$B_{dt}$	$9.7 \cdot 10^{-3}$	12.6	$2.1 \cdot 10^{-3}$	3656
	$P_{dt}$	$9.1 \cdot 10^{-4}$	4.0	$8.9 \cdot 10^{-6}$	3633
	$U^a$	-	-	-	-

<sup>a</sup> As Orig-ANN is sufficient to estimate  $U$ , using Log-ANN is unnecessary.

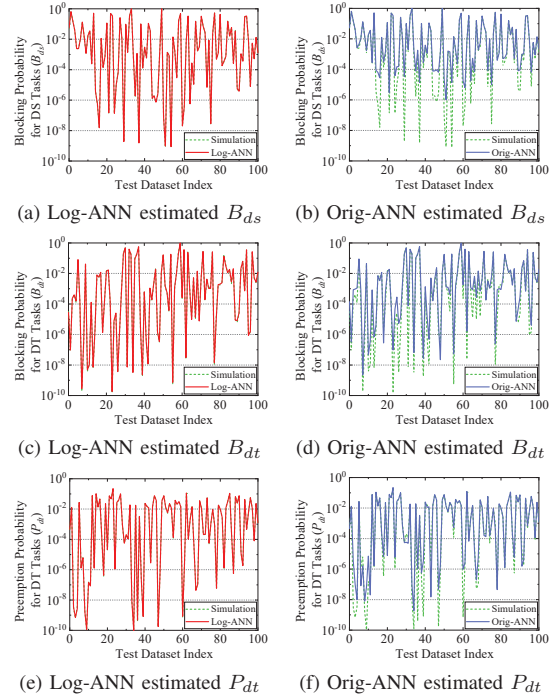


Fig. 3: Comparison among the simulation results, the Log-ANN estimations and the Orig-ANN estimations.

a one-neuron output layer. The MSE function is used as the loss function and the rectified linear unit (ReLU) activation function is used for the hidden layer. The ReLU activation function is used for the output layer. Note that the output of each model will be re-converted into the original forms to obtain the actual estimations of  $B_{ds}$ ,  $B_{dt}$  and  $P_{dt}$ . Let Log-ANN denote the ANN model with the logarithmic converting.

An ANN model is used to estimate  $U$ , which consists of a seven-neuron input layer, one hidden layer with 1500 neurons, and a one-neuron output layer. The MSE function is used as the loss function and the sigmoid activation function is used for both the hidden layer and the output layer. Let Orig-ANN denote the ANN model without the logarithmic converting.

In the training of both models, Adam optimizer with default parameters is used. 80% of the dataset is used as the training set and the remaining 20% is used as the test set. During the training process, 20% of the training samples are used as the validation set to avoid over-fitting. The early stopping criterion similar to Sect. III is used for both models.

Although MAE, MSE and MAPE are used to evaluate the estimation performance, neither MAE nor MSE is suitable for the evaluations, because their small values do not suggest a good estimation for the small values of the performance metrics. Compared with MAE and MSE, MAPE is a better measurement for the estimation error for the extremely small values. Orig-ANN is considered as a baseline model. Table II compares Log-ANN with Orig-ANN regarding the estimation performance. The results show that Log-ANN has lower MAPE than Orig-ANN. With the logarithmic converting, Log-

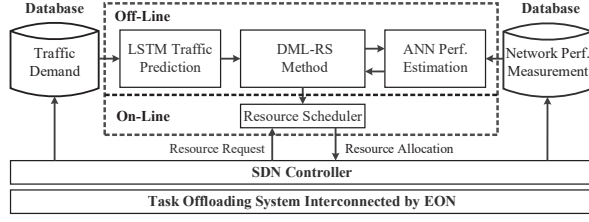


Fig. 4: Illustration of DML-RS for the task offloading system.

ANN can overcome the vanishing gradient issue and hence obtain faster convergence. On the other hand, with the logarithmic converting, a simpler ReLU function can be used as the activation function instead of the sigmoid function. Thus, Log-ANN needs less training time ( $t_{train}$ ) than Orig-ANN. Fig. 3 shows the comparisons among the simulation results, the Log-ANN estimations and the Orig-ANN estimations in terms of  $B_{ds}$ ,  $B_{dt}$  and  $P_{dt}$ . The Log-ANN models can obtain the estimation results similar to the simulation results. Compared with the Orig-ANN models, the Log-ANN models have higher accuracy on the estimations.

## V. RESOURCE SCHEDULING METHOD

Our idea is to schedule the resources in advance based on the predicted traffic variation in order to improve the performance while saving the spectrum resources. Here, we formulate the resource scheduling problem at the next  $t$  as an optimization model and present DML-RS to solve it. The overview of DML-RS is illustrated in Fig. 4.

### A. Problem Formulation

#### Given:

- $B_{ds}^{Max}$ ,  $B_{dt}^{Max}$ ,  $P_{dt}^{Max}$ : the upper bounds for  $B_{ds}$ ,  $B_{dt}$  and  $P_{dt}$  respectively based on the SLA made with the clients;
- $B_{ds}^{Min}$ ,  $B_{dt}^{Min}$ ,  $P_{dt}^{Min}$ : the lower bounds for  $B_{ds}$ ,  $B_{dt}$  and  $P_{dt}$  respectively based on the SLA made with the clients;
- $U^{Min}$ : the minimum  $U$  expected by the MEC operator;
- $S$ : the amount of storage capacity on an MEC server;
- $C$ : the amount of spectrum resources on an EON link;

#### Variables:

- $c_{ds}$ ,  $c_{dt}$ ,  $c_s$ : integer variables, denote the amount of spectrum resources assigned to the exclusive zone for either DS or DT tasks, and the shared zone;
- $s$ : integer variable, denotes the amount of storage resources assigned to DT tasks;

#### Objective:

$$\max \alpha \cdot \lg(B_{ds}) + \beta \cdot \lg(B_{dt}) + \gamma \cdot U \quad (1)$$

Our goals are twofold: i) minimizing  $B_{ds}$  and  $B_{dt}$  within the SLA-requested boundaries; ii) maximizing the bandwidth utilization. The objective function is formulated to achieve both the goals, as shown in Eq. (1). Let  $\alpha$ ,  $\beta$  and  $\gamma$  denote the weight factors to adjust the importance of the three terms. They can be specified by the MEC operators. Note that  $B_{ds}$ ,  $B_{dt}$ ,  $P_{dt}$  and  $U$  are functions of  $\lambda$ ,  $\delta$ ,  $\mu$ ,  $c_s$ ,  $c_{ds}$ ,  $c_{dt}$  and  $s$ .

### Algorithm 1 DML-RS Method

- 1: Input: the next network reconfiguration time point  $t$ , the physical distance between the MEC servers  $H$
- 2: Output: the allocation decision for  $t$
- 3: Initialize:  $obj \leftarrow 0$ ,  $CdsSet \leftarrow \emptyset$  and  $MaxObj \leftarrow \emptyset$
- 4: Use the LSTM model to predict  $\lambda_t$
- 5: Decide  $m$  and  $\mu$  based on  $H$
- 6: Given the predicted  $\lambda_t$ , search all the feasible amounts of spectrum resources (i.e.,  $C'$ ) that ensure  $B_{ds}$  satisfies Eq. (2) by using the Log-ANN-based  $B_{ds}$  estimation
- 7: Enumerate all possible combinations of  $\{c_{ds}, c_s\}$  that satisfy  $C' = c_{ds} + c_s$ , and store them in  $CdsSet$
- 8: **for all**  $\{c_{ds}, c_s\} \in CdsSet$  **do**
- 9:     **for all** possible combinations of  $\{c_{dt}, s\}$  that satisfy Eq. (6) and Eq. (7) **do**
- 10:         Find  $B_{dt}$ ,  $P_{dt}$  and  $U$  that satisfy Eq. (3), Eq. (4) and Eq. (5) respectively by using the Log-ANN-based  $B_{dt}$ ,  $P_{dt}$  and Orig-ANN-based  $U$  estimations
- 11:         Calculate Eq. (1) and obtain the resulting  $obj'$  based on the current  $\{c_{ds}, c_s, c_{dt}, s\}$
- 12:         **if**  $obj' \leq obj$  **then**
- 13:             Continue
- 14:         **else**
- 15:              $obj \leftarrow obj'$  and  $MaxObj \leftarrow \{c_{ds}, c_s, c_{dt}, s\}$
- 16:         **end if**
- 17:     **end for**
- 18: **end for**
- 19: **return** the optimal allocation decision  $\{c_{ds}, c_s, c_{dt}, s\}$

#### Constraints:

- 1) *Performance constraints.* Eq. (2), Eq. (3) and Eq. (4) ensure  $B_{ds}$ ,  $B_{dt}$  and  $P_{dt}$  are within the upper and lower bounds. Eq. (5) ensures the  $U$  is beyond its lower bound.

$$B_{ds}^{Min} \leq B_{ds} \leq B_{ds}^{Max} \quad (2)$$

$$B_{dt}^{Min} \leq B_{dt} \leq B_{dt}^{Max} \quad (3)$$

$$P_{dt}^{Min} \leq P_{dt} \leq P_{dt}^{Max} \quad (4)$$

$$U^{Min} \leq U \quad (5)$$

- 2) *Resource allocation.* Eq. (6) ensures the sum of spectrum resources pre-reserved for the offloading tasks cannot be more than  $C$ . Eq. (7) ensures the amount of storage assigned to DT tasks cannot be more than  $S$ .

$$c_{ds} + c_s + c_{dt} \leq C \quad (6)$$

$$0 \leq s \leq S \quad (7)$$

### B. Algorithm

Here, we present DML-RS. On one hand, DML-RS uses the LSTM model to predict  $\lambda_t$  at the next time point  $t$ . On the other hand, DML-RS uses the ANN models to estimate the metrics, given  $\lambda_t$  and a certain resource allocation. Finally,

TABLE III: Simulation Parameters

Parameter	Value	Parameter	Value	Parameter	Value
$C$	500 GHz	$S$	50 Gb	$F$	10 Gb
$H$	30 km	$B_{ds}^{Min}$	$10^{-7}$	$B_{ds}^{Max}$	$10^{-5}$
$B_{dt}^{Min}$	$10^{-7}$	$B_{dt}^{Max}$	$10^{-5}$	$P_{dt}^{Min}$	$10^{-4}$
$P_{dt}^{Max}$	$10^{-3}$	$U^{Min}$	0.2	$\delta$	0.2
$\alpha$	-1	$\beta$	-1	$\gamma$	50

DML-RS dynamically adjusts the resource allocation to optimize Eq. (1). Benefiting from the prediction, DML-RS can be initialized in advance before  $t$ . Thus, DML-RS is able to make timely decisions on scheduling.

Algorithm 1 presents the overall procedure of DML-RS. Line 4 uses the LSTM model to predict  $\lambda_t$ . Line 5 decides the modulation level  $m$  and  $\mu$  based on the transmission distance between the MEC servers. Line 6 searches all the feasible amounts of spectrum resources (i.e.,  $C'$ ) that ensure  $B_{ds}$  satisfies Eq. (2) by using the Log-ANN-based  $B_{ds}$  estimation, given  $\lambda_t$ . Line 7 enumerates all possible combinations of  $\{c_{ds}, c_s\}$  that satisfy  $C' = c_{ds} + c_s$ , and stores them in  $CdsSet$ . Line 10 finds a combination of  $\{c_{ds}, c_s, c_{dt}, s\}$  that satisfies Eq. (3), Eq. (4) and Eq. (5) using the Log-ANN-based  $B_{dt}$ ,  $P_{dt}$  and Orig-ANN-based  $U$  estimations. Line 11 calculates Eq. (1) and obtains  $obj'$  based on the current combination, where  $obj' = Eq. (1)$ . Lines 12-16 record  $obj'$  if  $obj'$  is larger than the previous  $obj$ . Line 19 returns the optimal allocation decision that maximizes Eq. (1).

## VI. RESULTS AND DISCUSSIONS

Simulation setup is listed in Table III. We compare DML-RS with two scheduling methods as follows. i) The optimal method has a prior knowledge of traffic variations and estimates the metrics based on extensive simulations. It searches an optimal decision in a greedy manner. ii) The ARIMA-OANN method uses the ARIMA traffic prediction and the Orig-ANN models to estimate all the metrics. It also greedily searches an optimal decision. The methods make the allocation decisions based on the predicted traffic demands. Based on the decisions, we run simulations to obtain the actual metrics.

Figs. 5 show the comparisons of the metrics among the three methods. Since DML-RS offers more accurate prediction and estimation than ARIMA-OANN, all the metrics in DML-RS meet the constraints and are close to the optimal method. However, in ARIMA-OANN, the performance upper or lower bounds are violated at multiple time points. This is because the ARIMA prediction is less accurate than our LSTM prediction and the Orig-ANN suffers from an over-estimation issue when the values of the metrics are extremely small. Besides, Fig. 5(d) compares the three methods with a static method. In this static method, the allocation decision is made based on the peak demand and remains unchanged over time. Compared with the static method, the dynamic scheduling methods can improve  $U$  significantly.

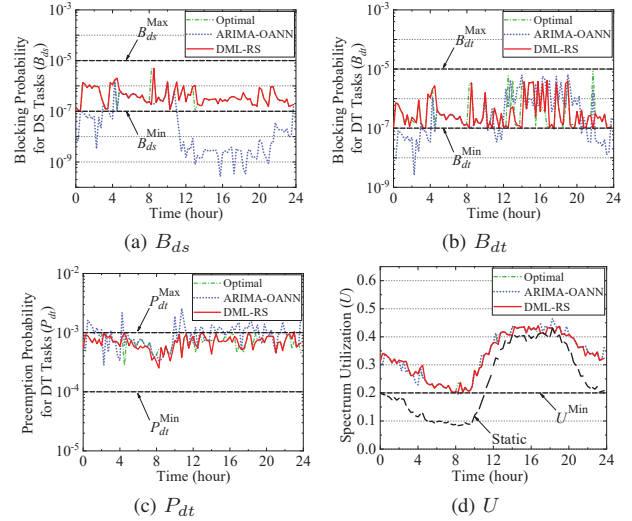


Fig. 5: Comparison among the resource scheduling methods.

## VII. CONCLUSIONS

In this paper, DML-RS is presented for data transfers in the task offloading system, which provides highly accurate traffic prediction and performance estimation. Simulations demonstrate that DML-RS achieves the results similar to the optimal method and outperforms ARIMA-OANN.

## REFERENCES

- [1] K. Ray and A. Banerjee, "A framework for analyzing resource allocation policies for multi-access edge computing," in *IEEE Int. Conf. Edge Computing (EDGE)*, pp. 102–110, 2021.
- [2] S. Huang, C. Yang, S. Yin, Z. Zhang, and Y. Chu, "Latency-aware task peer offloading on overloaded server in multi-access edge computing system interconnected by metro optical networks," *J. Lightwave Technol.*, vol. 38, no. 21, pp. 5949–5961, 2020.
- [3] M. Afrin, J. Jin, A. Rahman, A. Rahman, J. Wan, and E. Hossain, "Resource allocation and service provisioning in multi-agent cloud robotics: A comprehensive survey," *IEEE Commun. Surveys Tutorials*, pp. 1–26, 2021.
- [4] Y. Li, Z. Zeng, J. Li, B. Yan, Y. Zhao, and J. Zhang, "Distributed model training based on data parallelism in edge computing-enabled elastic optical networks," *IEEE Commun. Lett.*, vol. 25, no. 4, pp. 1241–1244, 2021.
- [5] W. Chu, P. Yu, Z. Yu, J. C. Lui, and Y. Lin, "Online optimal service selection, resource allocation and task offloading for multi-access edge computing: A utility-based approach," *IEEE Trans. Mob. Comput.*, pp. 1–18, 2022.
- [6] J. Shao, S. Zhang, W. Sun, and W. Hu, "Dimensioning access link capacity for time-varying traffic with mixed packet streams and circuit connections," *J. Opt. Commun. Netw.*, vol. 13, pp. 276–288, Nov 2021.
- [7] X. Lin, Y. Li, J. Shao, and Y. Li, "Storage-assisted optical upstream transport scheme for task offloading in multi-access edge computing," *J. Opt. Commun. Netw.*, vol. 14, pp. 140–152, Mar 2022.
- [8] V. Eramo, T. Catena, F. Lavacca, and F. di Giorgio, "Study and investigation of sarima-based traffic prediction models for the resource allocation in nfv networks with elastic optical interconnection," in *Int. Conf. Transparent Opt. Netw. (ICTON)*, pp. 1–4, 2020.
- [9] H. C. Leung, C. S. Leung, E. W. Wong, and S. Li, "Extreme learning machine for estimating blocking probability of bufferless obs/ops networks," *J. Opt. Commun. Netw.*, vol. 9, no. 8, pp. 682–692, 2017.
- [10] S. Mondal, G. Das, and E. Wong, "COMPASSION: A hybrid cloudlet placement framework over passive optical access networks," in *IEEE Conf. Comput. Commun. (INFOCOM)*, pp. 216–224, 2018.
- [11] <https://github.com/rankinjl/internet-traffic-stats-project>.